Progress In Electromagnetics Research Letters, Vol. 12, 161–170, 2009

THE EFFECT OF LOSS-TANGENT ON LADDERING BEHAVIOR IN DELAY LINES

A. Kabiri and M. B. Suwailam

Electrical and Computer Engineering
University of Waterloo
Waterloo, ON, Canada

M. H. Kermani

NetApp
Sunnyvale, CA, USA

O. M. Ramahi

Electrical and Computer Engineering
University of Waterloo
Waterloo, ON, Canada

Abstract—Delay lines come in varying topologies such as the simple meander line or the spiral delay lines. The major characteristic of these delay lines is their introduction of a laddering behavior at the output. Such laddering behavior can render the predictability of the delay very difficult unless time-consuming full-wave simulation is used. In previous works, delay lines were considered with minimal attention to the effect of the loss tangent. In this paper we have studied the effect of loss-tangent on the laddering behavior in delay lines and found that by considering the loss-tangent of the dielectric of the host medium, the laddering behavior is no longer present, thus eliminating the possibility of over- or under shooting logic levels at the output.

1. THEORETICAL BACKGROUND

There are two mechanisms that are typically employed to achieve required signal delay between circuit components. The first mechanism of delay is achieved through internal electronic circuitry. The second

Corresponding author: O. M. Ramahi (oramahi@ece.uwaterloo.ca).

mechanism, which is the most common and least expensive, is achieved through meandering a line as shown in Fig. 1. The meandered line, also referred to as the serpentine line, consists of a number of closely packed transmission lines. The objective behind the meandering is to achieve high density (of transmission line) per square mm of circuit board space while obtaining a delay in the signal that is directly proportional to the length of the line.

When serpentine lines are used in high-speed circuit applications, the time delay through a single serpentine line can be much larger than the rise time of the pulse. Under such conditions, serpentine lines have been found to introduce a spurious dispersion that makes the signal appears as if it is arriving earlier than would be expected based on the total electrical length of the line. This type of dispersion is caused by cross-talk between the adjacent transmission lines section, and is related to two parameters: the first is the length of each serpentine segment and the second parameter is the spacing between adjacent sections [1–3].

The coupling between two adjacent lines has been completely analyzed in previous works. If we consider the meander line plotted in Fig. 1, it is cumbersome to predict the total coupling and exact delay using an analytical method. From earlier simulation results, the interaction of these two parameters in conjunction with other line variables makes accurate prediction of the total skew generated by a particular design almost impossible without the use of full-wave electromagnetic simulators.

There is another important factor that has been ignored in previous works [1, 2]. Considering loss-tangent especially for high frequencies is crucial and we investigate its effect on laddering behavior.

2. WEAK COUPLING CROSS-TALK

A typical serpentine delay line is composed of closely packed transmission lines sections as shown in Fig. 1. Let us isolate two adjacent sections as shown in Fig. 2. After examination, we notice that the two isolated sections resemble the simplest case of two parallel

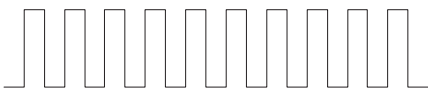

Figure 1. A typical meander line consisting of 10 segments.

Figure 2. One-turn serpentine line.

Figure 3. Parallel transmission lines with matched terminations. A pulse transmitted on the upper line generates cross-talk on the lower line that propagates in a manner equivalent to the case of the serpentine line segment shown in Fig. 2.

transmission lines [1]. After ignoring higher-order effects, the one-turn serpentine line shown in Fig. 2 is equivalent to the two transmission lines matched at both ends and shown in Fig. 3. Once this observation is made, using conventional transmission line analysis, one can predict the cross-talk induced on the second line due to the launched signal on the first line.

Considering Fig. 3, the near-end cross-talk, shown as voltage V_{NE}, is proportional to the mutual capacitance and mutual inductance characterizing the two lines. The cross-talk at the near and far ends can be written as

$$\begin{aligned} V_{NE}(t) &= k_{NE}\left[V_A(t) - V_A(t-2t_d)\right] \\ V_{FE}(t) &= k_{FE}t_d\frac{d}{dt}\left[V_A(t-t_d)\right] \end{aligned} \tag{1}$$

where t_d is the line delay and $V_A(t)$ is the voltage at the sending end of the active line. The proportional constants are

$$\begin{aligned} k_{NE} &= \frac{1}{4}(k_C + k_L) = \frac{1}{4}\left\{\frac{|C_{12}|}{C_{22}} + \frac{L_{12}}{L_{22}}\right\} \\ k_{FE} &= \frac{1}{2}(k_C - k_L) = \frac{1}{2}\left\{\frac{|C_{12}|}{C_{22}} - \frac{L_{12}}{L_{22}}\right\} \end{aligned} \tag{2}$$

and k_C and k_L are the capacitive and inductive coupling coefficients.

Let us assume that the rise time is smaller than the line delay, t_d. If a step function is launched on line 1, then the crosstalk at the near end of line 2 will be a pulse with duration twice the line delay (i.e., equivalent to the round-trip time). The crosstalk at the far end has a much smaller duration and it equals zero when the capacitive and inductive coupling coefficients are equal (as in the case when the medium is homogeneous as in strip lines). Since the pulse on the active line propagates to the right, the voltage at the near end of the passive line is in effect due to a leftward propagating wave. Similarly,

the voltage at the far end of the passive line is the accumulation of a rightward propagating wave (which is zero in the case of homogeneous medium).

If line 1, in Fig. 3, is excited by a pulse starting at $t = t_0$ and of duration T assumed to be shorter than the length of the line t_d, then the near-end crosstalk will consist of two opposite polarity pulses separated by $2t_d - T$, and each of duration T. This can be shown using the principle of superposition. By decomposing the finite duration input pulse into two opposite polarity step functions separated by T, the near-end crosstalk will be the sum of two pulses. The first pulse will have positive polarity and is excited at time t_0. The second pulse will have negative polarity and will start at time $t_0 + T$. The sum of the two pulses yields a waveform consisting of two pulses, each of duration T and separated by a time interval of width $2t_d - T$. This coupling mechanism is responsible for the synchronous or asynchronous coupling that takes place in the common delay lines reported in the literature [4].

3. CHARACTERIZATION OF DELAY LINES USING *S*-PARAMETER MEASUREMENTS

Three lines were considered in this work with all having a length of 41.59 cm and having stripline topology. The first is a test (control) line, the second a meander line and the thirds a spiral delay line, all shown in Figs. 4(a), (b) and (c), respectively. The three lines were fabricated on a single FR4 board. A photograph of the fabricated board is shown in Fig. 5. The S_{12} parameters were measured for the three lines and are shown in Figs. 5–7. S_{12} is observed to decrease rapidly for high frequencies. Since the line topology is a stripline, the rapid decrease in S_{12} is due to the loss tangent of the host dielectric.

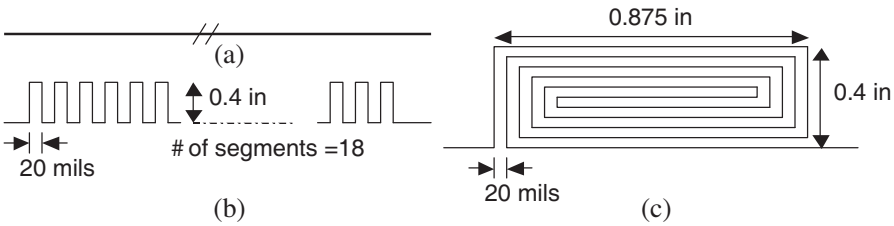

Figure 4. The three delay lines tested: (a) The test line, (b) The meander line, and (c) The spiral line. All three lines have an equal length of 41.59 cm.

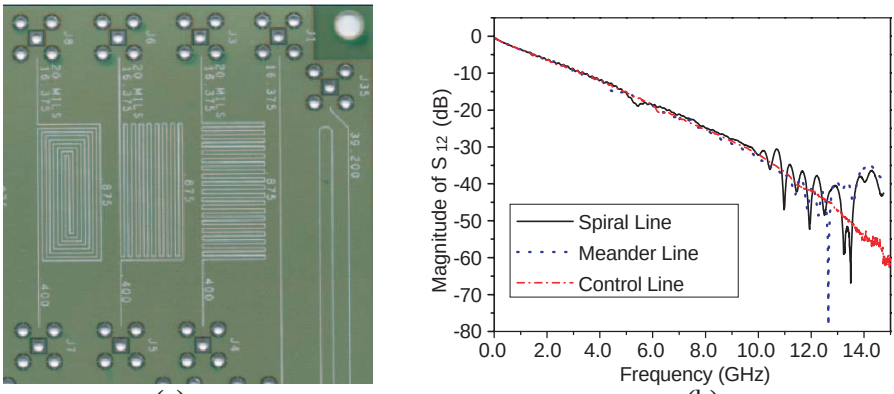

Figure 5. (a) Photo showing the fabricated board containing the different delay striplines. Notice that the lines are not visible but only traces to indicate their position within the fabricated board. The test line is partially shown. (b) Measured magnitude of S_{12}.

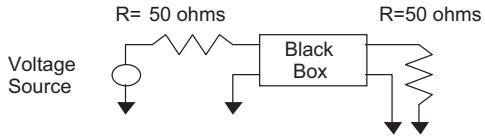

Figure 6. Schematic showing the numerical setup used to reconstruct the time-domain pulse response from the frequency domain measurements data. The black box represents the delay line under test.

Next, we use the measured S_{12} parameters to determine the time-domain response of each line using the simulation software Cadence [5]. The first step was to determine the characteristic impedance of the trace so that the proper load termination and source resistor could be used thus ensuring no reflection from the load, and that any signal distortion was due to the trace configuration. The circuit shown in Fig. 8 is used for time-domain simulation. There are two 50 Ohms resistors as source resistor and as termination resistor to avoid the distortion caused by mismatched load. The element specified as Black Box is the simulated delay line, which is characterized by its S-parameters.

A 1.4 nsec pulse with a 100 psec rise and fall time is used to excite the lines. It is important to mention that based on the excitation pulse (its rise-time, pulse-width and fall-time), it is necessary to

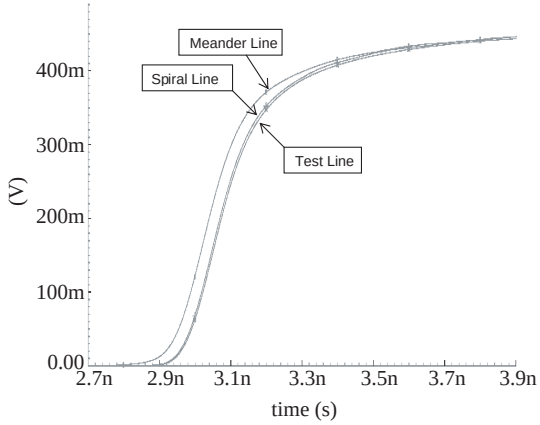

Figure 7. Time-domain response of the different delay lines reconstructed from the frequency domain measurements.

Figure 8. Cross section of the stripline.

have sufficient frequency range of the measured S-parameters. The simulation results are shown in Fig. 7. If we compare the shape of the received pulses with the theoretical results presented in [1–3, 4], it is clear that there is no laddering behavior in the received pulses. It is important, however, to note that even though the laddering is eliminated, the spiral line maintains its superiority to other delay line topologies in the sense that its behavior is the closest to the test (control) line which is a straight line.

In order to show the effect of loss-tangent on the laddering behavior, we first assume that the delay line is lossless (loss tangent = 0) and use Sonnet$^{\mathrm{R}}$ software [6]. Since Sonnet$^{\mathrm{R}}$ is a 2.5-dimensional full-wave software, it incorporates the entire coupling mechanism from the waveguide effects to the low-frequency capacitive and inductive couplings. For this simulation, the specific dimensions of the stripline

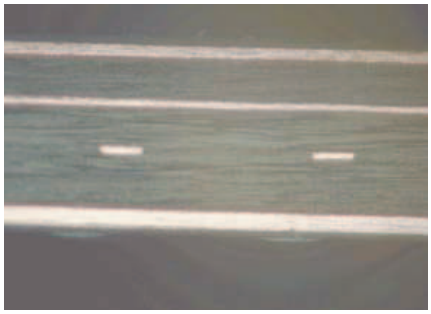

Figure 9. Fabricated board cross section showing the separation between adjacent traces and the location of the ground planes with respect to the traces.

are needed. These dimensions were obtained by cutting the board and taking photographs of the cross-section of the board which we present in Figs. 8 and 9. The line dimensions are obtained from the photographs directly. Summary of the topological dimensions is presented in Fig. 10.

We determined the relative dielectric constant and loss tangent of the board using formulas available in [7]. Based on our calculations the relative dielectric constant is 4.3. Since the loss tangent is a function of frequency, thus, in our simulation we divided the frequency range into two sections (0–8 GHz and 8–16 GHz). For the first frequency range we used an averaged measured loss tangent of 0.025 and for the second frequency range we used an averaged measured loss tangent of 0.045. The S_{12} parameter using both measurements and simulation is shown in Fig. 11. In fact, we observe very good agreement between the measurements and simulation.

For comparison of the time-domain behavior of the meander line, with and without dielectric losses, full-wave numerical simulations are provided here (note that it is not possible to construct a measurement setup where the losses of the dielectric board are zero). In the numerical simulation, we considered dielectric loss equivalent to that of the board tested above. We also used the same rise time of 100 psec considered to reconstruct the time-domain responses shown in Fig. 7. Fig. 12 shows the arriving pulse at the end of the line for the two cases (lossless and lossy). The simulation results presented in Fig. 12 were obtained using the three-dimensional full-wave numerical simulation tool Microwave Studio CST [8]. In this simulation, the center conductor of the strip line and the conductors of the reference planes were assumed to have zero thickness and infinite conductivity.

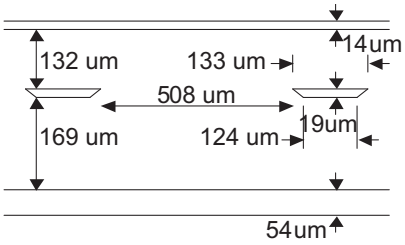

Figure 10. Cross section of the strip line showing dimensions corresponding to the fabricated board.

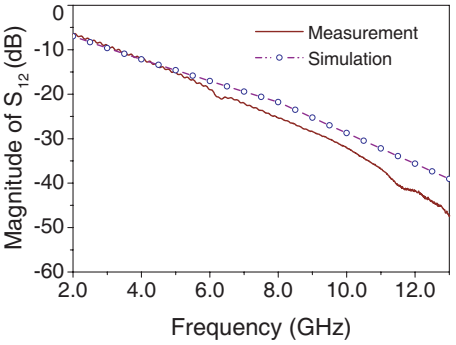

Figure 11. Measurement and simulation results for the test meander line. In the simulation, a loss tangent of 0.025 and 0.045 was used for the frequency ranges 0–8 GHz and 8–16 GHz, respectively.

Since there are errors inherent in our determination of the dielectric constant and especially the loss tangent, in Fig. 13, we show the response of the meander line for the lossless and lossy cases, but this time, the losses have been increased to 0.05 and 0.09 for the frequency ranges 0–8 GHz and 8–16 GHz, respectively. This simulation (Fig. 13) is intended to give a very qualitative perspective on the effect of having higher losses in the transmission line system. Clearly observed, from the results presented in Fig. 13, that as the losses of the transmission line system increase, the more the output pulse deviates from that of the ladder-dominated response that characterizes the lossless system. Notice the DC offset seen before the arrival of the pulse (in Figs. 12 and 13) is a typical characteristic of the meander line and is due to the synchronous coupling that results in premature arrival of some pulse energy.

Finally, we emphasize that the time-domain responses of the different transmission lines (see Fig. 7) were reconstructed from the frequency domain measurements. The reconstruction setup (as discussed above and schematically exhibited in Fig. 6), assumes perfect voltage source and frequency-independent 50 Ohms impedance terminations. This will not be the case in three-dimensional full-wave simulations which account for some of the discrepancies between the full-wave simulation results and the reconstructed timedomain data based on frequency domain measurements.

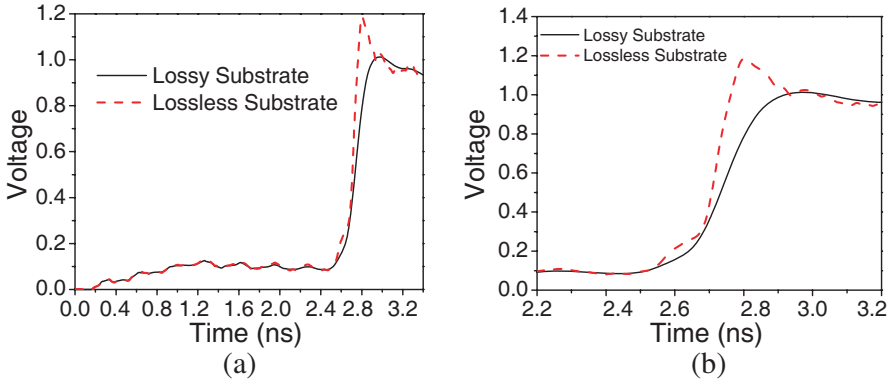

Figure 12. Full-wave three-dimensional numerical simulation showing the meander delay line time-domain response. In the simulation, a loss tangent of 0.025 and 0.045 was used for the frequency ranges 0–8 GHz and 8–16 GHz, respectively. (a) Extended time scale to show the onset of the pulse arrival. (b) Expanded time scale to show the effect of loss.

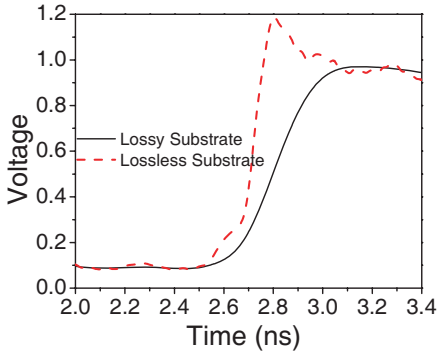

Figure 13. Full-wave three-dimensional numerical simulation showing the meander delay line time-domain response. In the simulation, a loss tangent of 0.05 and 0.09 was used for the frequency ranges 0–8 GHz and 8–16 GHz, respectively.

4. CONCLUSION

Laddering behavior in delay lines is due to the coupling between adjacent lines. The coupling is proportional to the mutual capacitance and mutual inductance characterizing the two lines and it is considerable when the signal includes high frequency components. When the high frequency components are attenuated significantly, the

laddering behavior is no longer manifested. As a result, the possibility of over- or under-shooting the logic voltage levels at the output are minimized or even eliminated altogether, thus maintaining the signal integrity and eliminating electromagnetic interference potential.

REFERENCES

1. Wu, R. and F. Chao, "Laddering wave in serpentine delay line," *IEEE Trans. on Components, Packaging, and Manufacturing Technology — Part B*, Vol. 18, No. 4, Nov. 1995.
2. Wu, R. and F. Chao, "Flat spiral delay line design with minimum crosstalk penalty," *IEEE Trans. on Components, Packaging, and Manufacturing Technology — Part B*, Vol. 19, No. 2, May 1996.
3. Rubin, B. J. and B. Singh, "Study of meander line delay in circuit boards," *IEEE Trans. on Microwave Theory and Techniques*, Vol. 48, No. 9, Sep. 2000.
4. Ramahi, O. M., "Analysis of conventional and novel delay lines: A numerical study," *Journal of Applied Computational Electromagnetic Society*, Vol. 18, No. 3, 181–190, Nov. 2003.
5. CADENCE IC4.4.6, Cadence Design Systems, San Jose, CA, USA.
6. SONNET Version 7.0, Sonnet Software, Inc., Liverpool, NY, US.
7. Collin, R. E., *Foundations for Microwave Engineering*, The IEEE Press Series on Electromagnetic Wave Theory, 2001.
8. Microwave Studio, CST of America, Inc., Framingham, MA, USA.